



Recent changes in thickness of the Devon Island ice cap, Canada

David Burgess^{1,2} and Martin J. Sharp¹

Received 19 June 2007; revised 28 March 2008; accepted 8 April 2008; published 19 July 2008.

[1] Long-term rates of thickness change were derived at several spatial scales using a variety of methods for most of the Devon Island ice cap, Nunavut, Canada. Basin-wide thickness change calculations were derived for the accumulation zones of all major drainage basins as the area-averaged volume difference between balance and InSar fluxes at the altitude of the long-term equilibrium line (ELA). Thickness changes for ablation zones were derived as a function of the surface mass balance, flux across the EL and calving flux, averaged across the ablation areas. Average rates of thickness change are near zero in the accumulation zones of the northern and southwestern basins but reach $-0.23 \pm 0.11 \text{ m a}^{-1}$ w.e. in the southeast basin due to dynamic thinning. Thickness changes were also estimated along five major outlet glaciers as a function of flux divergence and net surface mass balance and along the Belcher Glacier by comparing elevation values derived from 1960s aerial photography with those derived from 2005 NASA Airborne Topographic Mapper (ATM) surveys. Ice dynamics have had a significant influence on the pattern of thickness change of all outlet glaciers examined in this study. Volume changes derived from the basin-wide values indicate a net loss of $-76.8 \pm 7 \text{ km}^3$ water equivalent from the main portion of the ice cap from 1960 to 1999, contributing $0.21 \pm 0.02 \text{ mm}$ to global sea level over this time. This value is $\sim 44\%$ greater than previous estimates of volume change based on volume-area scaling methods and surface mass balance alone.

Citation: Burgess, D., and M. J. Sharp (2008), Recent changes in thickness of the Devon Island ice cap, Canada, *J. Geophys. Res.*, 113, B07204, doi:10.1029/2007JB005238.

1. Introduction

[2] Knowledge of the rates of thickness change of the Earth's large ice masses is crucial to understanding their state of balance and contribution to global sea level change. Combined, the Greenland and Antarctic ice sheets would raise sea level by $>80 \text{ m}$ if they were to disintegrate completely. Smaller ice caps and glaciers pose a more immediate concern, however, and may have accounted for a significant fraction ($>50\%$) of total sea level rise over the last century [Dyurgerov and Meier, 2005]. Currently, model predictions of volume loss from these ice masses are based on changes in surface mass balance alone [Intergovernmental Panel on Climate Change (IPCC), 2007]. Recent studies have, however, demonstrated that climate induced changes in ice dynamics can significantly influence the net mass balance of high-latitude ice masses [Rignot and Kanagaratnam, 2006]. It is therefore essential to determine the relative impact of changes in ice dynamics, iceberg calving, and surface mass balance in order to properly assess how large ice masses in the polar regions may respond to future climate warming.

[3] The Devon Island ice cap occupies approximately $14,000 \text{ km}^2$ of the eastern half of Devon Island, Nunavut (Figure 1), which makes it one of the largest ice masses in

the Canadian high Arctic. This ice cap derives a significant proportion of its accumulation from the North Open Water Polynya in Baffin Bay [Koerner, 1977]. According to field measurements collected by R. Koerner, the net mass balance of the northwest sector of the Devon Island ice cap (Figure 2) over the period 1961–2001 was -0.086 m a^{-1} water equivalent (w.e.). Interannual variations in net mass balance on the ice cap arise mainly from variations in the summer balance [Koerner, 2002].

[4] One estimate of volume change of the Devon Island ice cap, which is based on in situ mass balance data collected in the northwest sector of the ice cap by R. Koerner between 1961 and 2003, indicates that the main part of the ice cap has decreased in volume by $\sim 42 \text{ km}^3$ w.e. This value is a minimum estimate however, as it does not account for losses due to iceberg calving. An independent volume loss estimate of $-0.81 \text{ km}^3 \text{ a}^{-1}$ (of ice) was derived from surface elevation changes measured from repeat laser altimetry performed by NASA in 1995 and 2000 (lines NASA_EW1, NASA_EW2, and NASA_NS1; Figure 2) [Abdalati et al., 2004]. This yields a total loss of -31 km^3 w.e. when extrapolated over the 42 year period. Both sets of observations are of limited value in terms of estimating volume change for the Devon Island ice cap as a whole due to the large extrapolations involved.

[5] Comparison of the ice margins identified on 1960 aerial photography and on 1999 Landsat7 ETM+ imagery reveals significant spatial variability in the rate and sign of fluctuations of the margins of the Devon Island ice cap

¹Department of Earth and Atmospheric Sciences, University of Alberta, Edmonton, Alberta, Canada.

²Now at Canada Centre for Remote Sensing, Ottawa, Ontario, Canada.

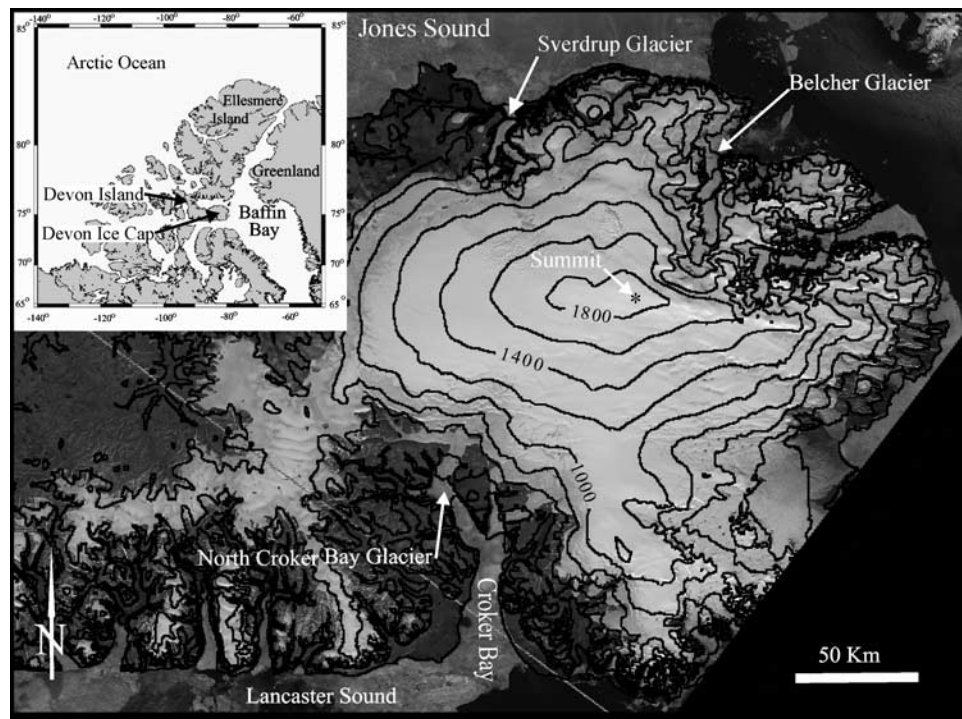


Figure 1. 1999 Landsat 7 ETM+ orthomosaic of the Devon ice cap, Nunavut, Canada. Inset shows the location of the Devon ice cap in the Canadian Arctic Archipelago.

[Burgess and Sharp, 2004]. The dominant changes identified include retreat of most of the larger tidewater glaciers (by as much as 3 km in the southeast region) and advance of the western margin by up to 120 m. The net volume decrease of the main ice cap (excluding the stagnant southwest arm) was estimated to be $-44 \pm 5 \text{ km}^3$ w.e. using volume-area scaling techniques [Burgess and Sharp, 2004]. Using a combination of ice core derived estimates of net accumulation and melt modeling, Mair *et al.* [2005] estimated the net volume reduction of the ice cap to be $-59 \pm 26 \text{ km}^3$ w.e. between 1963 and 2000 due to net surface mass balance alone. They identified the southeast region as the area where the greatest volume changes are occurring. Combined with mass loss due to iceberg calving ($-19 \pm 5 \text{ km}^3$ water equivalent between 1960 and 1999) [Burgess *et al.*, 2005], it is estimated that total loss from the Devon Island ice cap over the past 40 years may be as great as -78 km^3 water equivalent. It seems likely that there is significant variability in the magnitude and sign of volume change across the Devon Island ice cap, and accounting for this variability results in estimates of volume change that are consistently larger than those derived from “localized” mass balance observations and altimetry.

[6] In this study, estimates of the long-term (40 years) rates of thickness change of the Devon Island ice cap, Nunavut, Canada, are derived using several approaches. First, average rates of thickness change were calculated for the accumulation zones of individual drainage basins as the area weighted difference between the measured ice flux and balance flux at the altitude of the equilibrium line (ELA). For the ablation zones of these basins, average rates of thickness change were calculated from the difference between the mass flux at the ELA and the sum of the volume

losses from the ablation area by surface mass balance and iceberg calving. Second, in situ measurements of rates of thickness change were obtained for three sites in the southwest region of the ice cap using (1) the “coffee can” technique developed by Hamilton and Whillans [2000] and (2) measurements of the 40 year surface mass balance and vertical strain across a $1 \text{ km} \times 1 \text{ km}$ grid. Third, rates of thickness change along five major outlet glaciers (the Fitzroy, North and South Croker Bay, and the Southeast 1 and 2 Glaciers) were derived as a function of the difference in ice flux between successive gates spaced 5–8 km apart, and the average net surface mass balance between the fluxgates. For the Belcher Glacier only, direct measurements of surface lowering were obtained by comparing surface elevations obtained from analytical stereo photogrammetry from 1960s aerial photography with values obtained from an airborne laser altimetry survey conducted by NASA in the spring of 2005.

[7] These measurements should allow us to answer important questions concerning the state of balance of the Devon Island ice cap. These include: (1) What is the magnitude of volume loss from the ice cap since 1960 and how much does this contribute to global sea level change? (2) How is volume change distributed between drainage basins? (3) Is area change at the scale of individual drainage basins a good guide to volume change? (4) How is volume change distributed between the accumulation and ablation zones? (5) Are there distinctive longitudinal patterns of elevation change along outlet glaciers, and how do these patterns compare with those at the basin-wide scale? (6) Is there evidence from the patterns of thickness change, either within whole basins or along outlet glaciers, for recent changes in flow dynamics that have resulted in rates

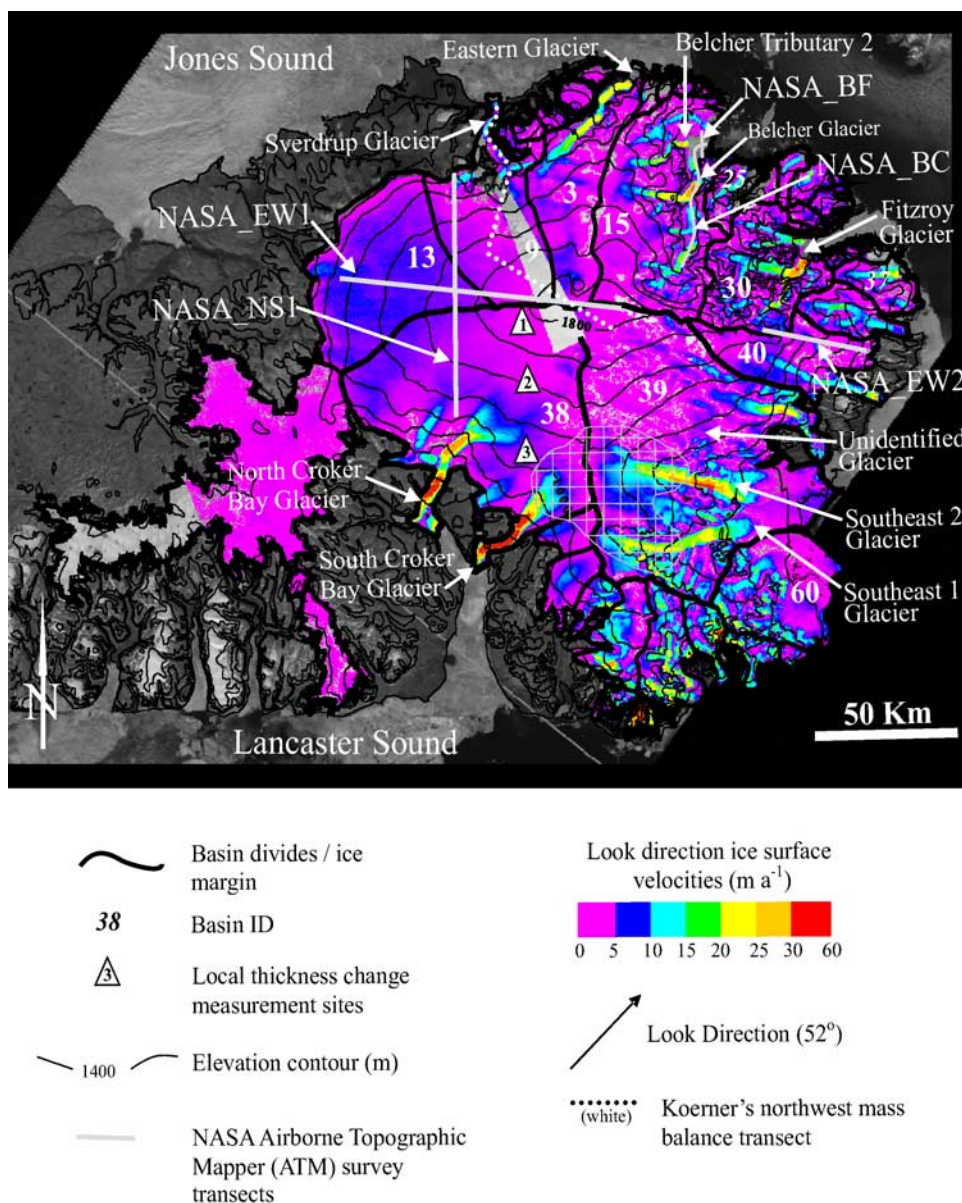


Figure 2. InSAR look direction surface velocities across the Devon Ice Cap derived from the ERS 1/2 satellite data. The gray gridded area in the southern region of the ice cap indicates the location where surface accumulation rates were increased by 1.5 times the amount derived by *Mair et al.* [2005].

of thinning/thickening that are not easily accounted for by changes in surface mass balance alone?

2. Data Sets

[8] Calculations of rates of thickness change were made possible by the recent development of ice thickness, topography, surface mass balance, and ice surface velocity data sets for the Devon Island ice cap. Ice thickness data across most of the ice cap were derived from airborne radio echo sounding measurements obtained during the spring of 2000 [Dowdeswell et al., 2004]. These data are accurate to ± 10 m, whereas the ice surface elevation values are accurate to ± 7 m. Surface mass balance data for the accumulation zone were derived from interpolation of long-term net accumulation rates measured at eight sites in the accumulation area

of the ice cap. Net accumulation at each site was determined using down-borehole ^{137}Cs gamma ray spectrometry to detect the depth to the 1963 “bomb” layer that was deposited as fallout from atmospheric thermonuclear weapons testing in the Russian high Arctic in 1962 [Mair et al., 2005]. Mean net accumulation rates over the 37-year period (1963–2000) were calculated as a function of depth to the reference layer and the density of the overlying firn. On the basis of field measurements of net accumulation performed at three sites in the southern region of the ice cap in Spring 2005, the accumulation grid developed by *Mair et al.* [2005] was modified to take into account accumulation rates that locally exceeded those shown by *Mair et al.* [2005] by a factor of 1.5. The area affected encompassed the source regions of the South Croker Bay, Southeast 1, and Southeast 2 Glaciers (see Figure 2). This modifica-

tion had the effect of raising the mass balance of basin 38 by 2.5% and basin 39 by 6%, resulting in a net increase of $0.017 \text{ km}^3 \text{ a}^{-1}$ in the mass balance of the whole ice cap. For the ablation zone, the net balance was calculated using a positive degree-day model driven by air temperature data from Resolute Bay, Nunavut, corrected for conditions specific to the ice cap [Mair *et al.*, 2005]. Surface velocity fields for the ice cap were derived by satellite radar interferometry (InSAR) using ascending pass ERS 1 and 2 data obtained during the tandem mode mission in the spring of 1996 and the 3-day repeat pass mission in February 1992 [Burgess *et al.*, 2005]. Errors associated with these data are $\pm 3 \text{ m a}^{-1}$ throughout the interior regions of the ice cap, and from 10% to 30% of the measured velocity along the fast flowing outlet glaciers, depending on the angle between the satellite look direction and the direction of ice flow. Since these data represent ice velocities over a 1–3 day time interval, uncertainties related to possible temporal variations in flow rates also exist when comparing InSAR derived ice fluxes with balance flux values derived from the 37 year accumulation values as described above. The lack of data on seasonal variability in rates of flow of the Devon Island ice cap precludes us from quantifying this uncertainty. Finally, the surface topography of the ice cap was obtained from the Canadian Digital Elevation Data set (CDED) with a horizontal resolution of 100 m. It was produced from 1:60,000 aerial photography acquired in 1959–1960 by the Government of Canada. Errors associated with limited bedrock control, problems with photogrammetric data capture over low contrast regions, and conversion of data from analog to digital format result in surface elevation errors of $\pm 50 \text{ m}$ along the main outlet glaciers and up to $\pm 100 \text{ m}$ throughout the ice cap interior. These errors are considered random at the ice cap-wide scale. A second DEM of the Belcher Glacier, with a grid cell resolution of 20 m, was recently produced from this photography. Ground control points obtained from differential GPS (DGPS) measurements in the spring of 2005 indicate that these raw data are accurate to $\pm 2 \text{ m}$ in the vertical and $\pm 1 \text{ m}$ in the horizontal dimensions. Along- and cross-profiles of surface and bed elevation of the Belcher Glacier were also obtained in 2005 from NASA's Airborne Topographic Mapper (ATM) and the University of Kansas Coherent Radar Depth Sounder (CoRDS), respectively (lines NASA_BC and NASA_BF; Figure 2) [Krabill *et al.*, 2006]. Vertical resolutions of the ATM and CoRDS data are $\pm 10 \text{ cm}$ and $\pm 10 \text{ m}$, respectively.

3. Methods

3.1. Basin-Wide Thickness Changes

[9] Average rates of thickness change were calculated for the accumulation and ablation zones of 10 major ($>100 \text{ km}^2$) drainage basins, excluding the western lobe of the ice cap, for which InSAR derived surface velocities are sparse. Basins for which the accumulation area comprises $<5\%$ of the total basin area (basins 60, 37, and 25) were considered to consist of ablation zones only.

[10] For the accumulation zone, the mean rate of thickness change was calculated from the difference between the

balance and observed water equivalent flux values (Q_{Balance} and Q_{InSAR} , respectively) across the ELA:

$$\partial H / \partial t_{\text{acc}} = ((Q_{\text{Balance}} - Q_{\text{InSAR}}) / A_{\text{acc}}) \quad (1)$$

where

$$Q_{\text{balance}} = HV_{\text{Balance}} \text{ ELA}_{\text{length}} \quad (2)$$

and

$$Q_{\text{InSAR}} = HV_{\text{InSAR}} \text{ ELA}_{\text{length}} \quad (3)$$

V_{balance} is the balance velocity (the depth averaged flow rate required to maintain profile equilibrium in an ice mass; km a^{-1}) [Paterson, 1994] and A_{acc} is the area of the accumulation zone within a particular basin (km^2). V_{InSAR} is the depth averaged velocity derived by applying a correction value (explained below) to the surface velocity measured from satellite radar interferometry (km a^{-1}) [Burgess *et al.*, 2005]. HV_{InSAR} (HV_{balance}) ($\text{km}^2 \text{ a}^{-1}$) is the average for all grid cells along the ELA within a particular basin, where the value for each grid cell is the product of V_{InSAR} (V_{Balance}) and ice thickness (H) (km) in that grid cell. The long-term ELA was estimated as 950 m a.s.l. for the northwest, 800 m a.s.l. for the southeast, and 875 m a.s.l. for both the northeast and southwest regions [after Koerner, 1970]. The boundaries of these regions are indicated in Figure 3.

[11] V_{balance} was derived from the model of Budd and Warner [1996] using surface mass balance [Mair *et al.*, 2005] modified as described above, ice thickness [Dowdeswell *et al.*, 2004], and surface topography (CDED), as input data. The pattern of glacier flow produced by the balance velocity model (Figure 4) closely reflects the InSAR-derived flow pattern (Figure 2), with the exception of four flow features that are not observed in the InSAR data (identified as A, B, C, and D in Figure 4). Since these features are embedded within much larger drainage basins, the misrouting of flow along them would not affect balance flux calculations at the basin scale. Flow unit A, however, appears to divert modeled flux from the South Croker Bay Glacier. Flow unit D is located in the southeast region and drains directly south from the summit region to join up with the Southeast 2 Glacier approximately 30 km up glacier from its terminus. Discontinuous patches of enhanced velocity in the InSAR data along the path of this feature support the existence of a major flow unit in this area (unidentified glacier; Figure 2). It is likely that this feature was not fully resolved by the InSAR data because ice flow in this region is nearly perpendicular to the look angle of the satellite (52°). Despite these differences, the overall similarity between the flow structures produced by the balance velocity model and the InSAR measurements provides confidence in the comparability of these data.

[12] In order to make V_{InSAR} , which is a surface quantity, compatible with V_{balance} , which is a depth-averaged quantity, V_{InSAR} was multiplied by 0.8 over regions where the predominant mode of ice flow is inferred to be by internal

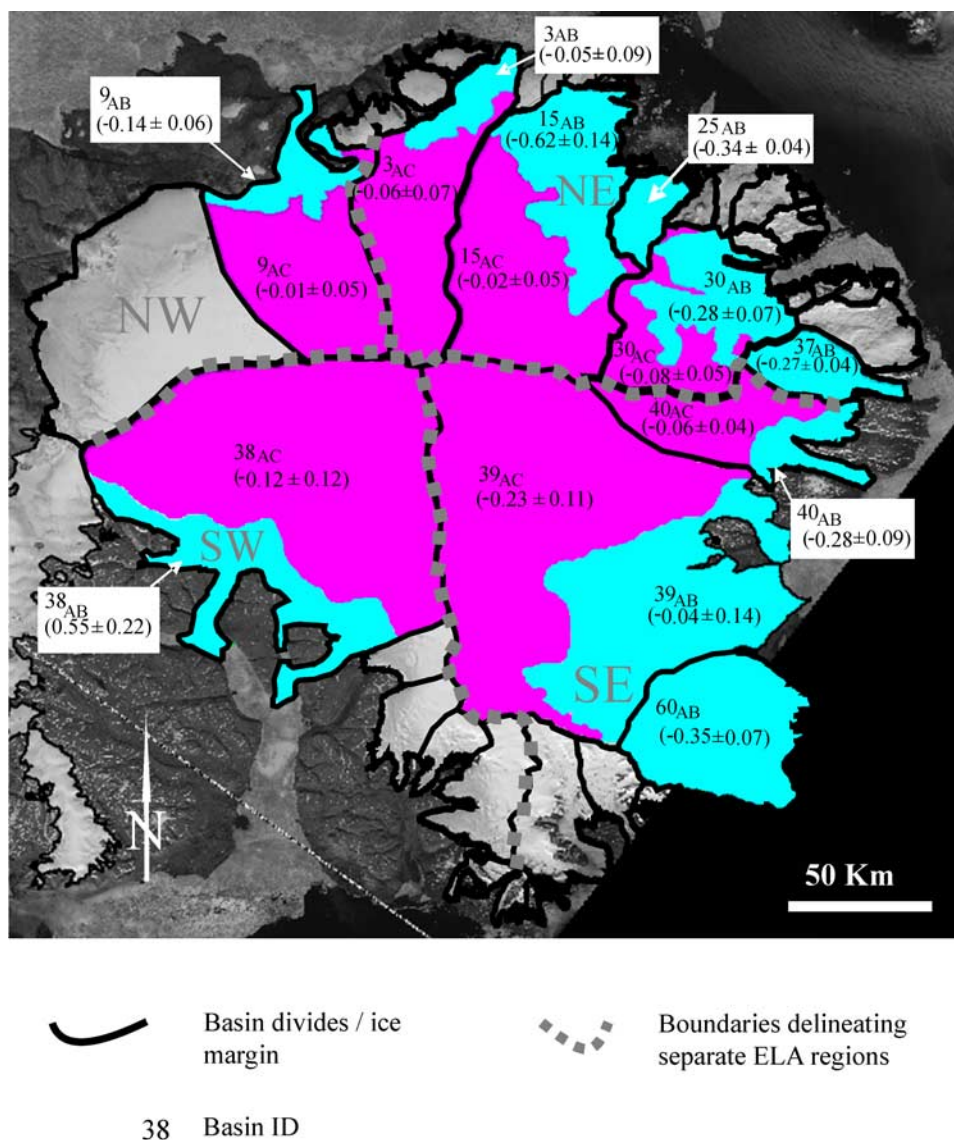


Figure 3. Basin-wide thickness changes of the accumulation (AC) and ablation (AB) zones of the Devon Island ice cap (m a^{-1} w.e.). The ELA is specified to be 950 m in northwest (NW), 800 m in the southeast (SE), and 875 m in the southwest (SW) and northeast (NE) quadrants [Koerner, 1970]. Light blue represents the ablation zone and purple the accumulation zone.

deformation. This value is a conservative approximation based on the ratio of surface velocity to velocity measurements at depth measured near the summit of the Devon Island ice cap by Reeh and Paterson [1988]. V_{InSAR} was assumed to be equal to the depth-averaged velocity in areas where sliding is inferred to be the predominant mode of ice flow [Burgess *et al.*, 2005]. Although internal deformation may still occur where basal sliding dominates, this contribution is expected to be small (<5%) relative to the uncertainties in the InSAR-derived surface velocities (15–20%), which are accounted for in the calculations of ice flux. Inferences of whether ice movement is predominantly by internal deformation or sliding are based on an analysis of the relationship between the ratio of velocity to ice thickness (V/H) and the driving stress [Burgess *et al.*, 2005].

[13] The uncertainty (σ) associated with the application of equation (1) to each basin was estimated as:

$$\sigma(\partial H/\partial t_{\text{acc}}) = \left(\sqrt{(\sigma(Q_{\text{balance}}))^2 + (\sigma(Q_{\text{InSAR}}))^2} \right) / A_{\text{acc}} \quad (4)$$

where $\sigma Q_{\text{balance}}$ (and σQ_{InSAR}) was calculated as the difference between an upper estimate of flux ($Q_{\text{balance_upper}}$ (and $Q_{\text{InSAR_upper}}$)), and the best estimate of flux (Q_{balance} (and Q_{InSAR})) (see Table 1). $Q_{\text{balance_upper}}$ was derived as the product of the upper estimate of ice thickness ($H_{+10\text{m}}$) and $V_{\text{balance_upper}}$, where $V_{\text{balance_upper}}$ was produced from the balance flux model using upper estimates of net surface mass balance ($b + \sigma b$) [Mair *et al.*, 2005]. $Q_{\text{InSAR_upper}}$ was derived as the product of $H_{+10\text{m}}$ and $V_{\text{InSAR_upper}}$, where $V_{\text{InSAR_upper}}$ was derived by adding the estimated ice

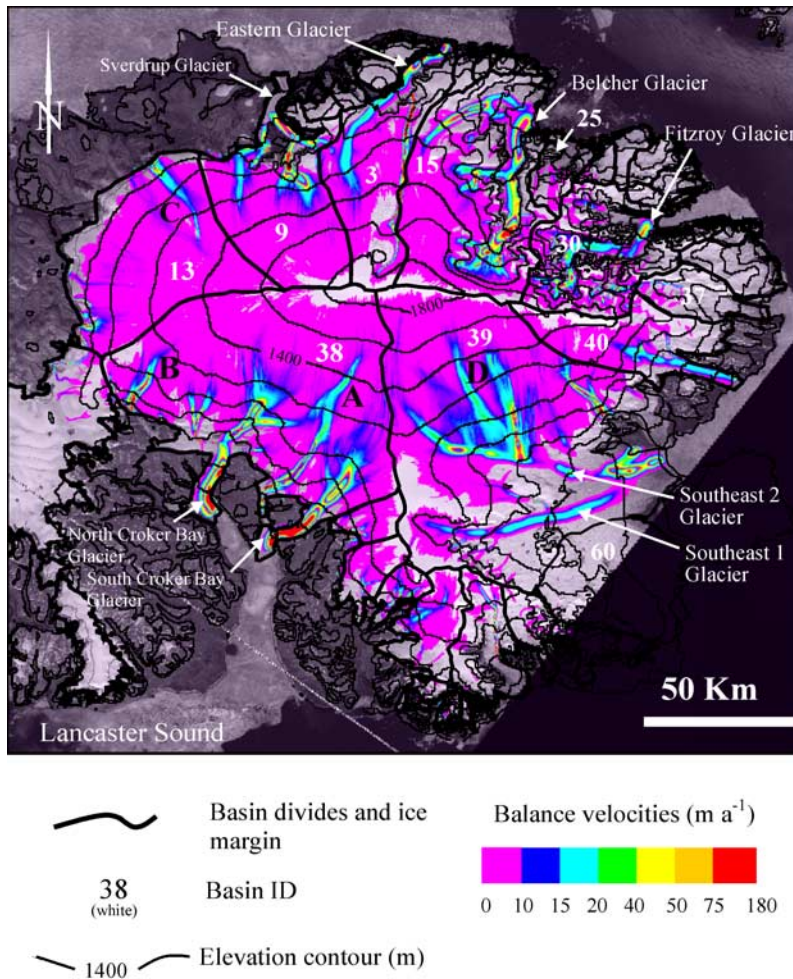


Figure 4. Modeled balance velocities across the Devon Island ice cap. Areas of missing data represent sections of the ice cap where the modeled balance velocity is less than 1 m a^{-1} . Flow units not evident in the InSAR derived velocity fields are indicated as A, B, C, and D.

velocity error (specified in the work of Burgess *et al.* [2005]), to V_{InSAR} . Error associated with A_{acc} had a negligible effect on the final value of $\partial H/\partial t_{\text{acc}}$.

[14] For the ablation zones, the average rate of thickness change in water equivalent was calculated from the differ-

ence between the measured flux across the ELA and the sum of the mass loss rates by surface ablation and calving:

$$\partial H/\partial t_{\text{abl}} = (Q_{\text{InSAR}} + Q_{\text{abl}} + Q_{\text{calving}})/\text{Area}_{\text{abl}} \quad (5)$$

Table 1. Rates of Water Equivalent Volume Change Throughout the Accumulation and Ablation Zones of the Major Tidewater Terminating Basins Across the Devon Island Ice Cap^a

Basin ID	Accumulation Zone		Ablation Zone		
	Net Volume Change ($\text{km}^3 \text{ a}^{-1} \text{ w.e.}$)	Net Volume Change ($\text{km}^3 \text{ a}^{-1} \text{ w.e.}$)	Measured Flux at the ELA ($\text{km}^3 \text{ a}^{-1} \text{ w.e.}$)	Surface Mass Balance ($\text{km}^3 \text{ a}^{-1} \text{ w.e.}$)	Calving Flux ($\text{km}^3 \text{ a}^{-1} \text{ w.e.}$)
3	-0.036 ± 0.020	-0.017 ± 0.024	0.089	-0.075	-0.028
9	-0.003 ± 0.025	-0.046 ± 0.016	0.058	-0.092	-0.011
15	-0.013 ± 0.031	-0.274 ± 0.070	0.074	-0.162	-0.21
25	n/a	-0.045 ± 0.006	n/a	-0.041	-0.003
30	-0.029 ± 0.013	-0.08 ± 0.026	0.059	-0.104	-0.032
37	n/a	-0.053 ± 0.008	n/a	-0.051	-0.002
38	-0.213 ± 0.180	0.357 ± 0.111	0.479	-0.072	-0.046
39	-0.385 ± 0.137	-0.114 ± 0.142	0.512	-0.606	-0.018
40	-0.018 ± 0.010	-0.046 ± 0.141	0.027	-0.066	-0.006
60	n/a	-0.532 ± 0.042	n/a	-0.528	-0.003

^aNet volume change of the accumulation zone represents the difference between balance and observed flux at the ELA. Individual components contributing to net volume change of the ablation zone are shown separately.

where Q_{abl} (see Table 1) is the volumetric net surface balance of the ablation zone as obtained from *Mair et al.* [2005], $Q_{calving}$ (see Table 1) is the water equivalent mass lost by iceberg calving as computed by *Burgess et al.* [2005], and $Area_{abl}$ is the total area of the ablation zone in 1999. As indicated in Table 1, mass loss rates due to net surface ablation and iceberg calving are negative values.

[15] Since a positive net balance could have the effect of glacier advance as well as thickening, the apparent thickness change estimate for a basin in which the ice cap was growing was adjusted by the formula:

$$\partial H / \partial t_{abLadvance} = \partial H / \partial t_{abl} - (Q_{adv} / Area_{abl}) \quad (6)$$

where Q_{adv} is the average annual rate of volume increase due to glacier advance in the basin since 1960 [*Burgess and Sharp*, 2004]. This correction factor was applied to basin 38, which is the only sector of the ablation zone that has experienced net growth over the past 40 years.

[16] The total error associated with equation (5) was calculated as:

$$\sigma(\partial H / \partial t_{abl}) = \left(\frac{\sqrt{(\sigma(Q_{InSAR}))^2 + (\sigma(Q_{abl}))^2 + (\sigma(Q_{calving}))^2)}}{Area_{abl}} \right) \quad (7)$$

where σQ_{abl} was obtained from *Mair et al.* [2005] and $\sigma Q_{calving}$ was obtained from *Burgess et al.* [2005]. Errors in $Area_{abl}$ had an insignificant effect on the estimate of $\sigma(\partial H / \partial t_{abl})$.

3.2. In Situ Measurements of Rates of Ice Thickness Change

[17] In situ measurements of rates of ice thickness change were made at three locations in the southwest region of the ice cap in 2004 and 2005 (site 1, 1800 m; site 2, 1400 m; and site 3, 1000 m a.s.l.; see Figure 2 for locations). These measurements, which were derived using two separate methods, provide independent checks on estimates produced using remote sensing techniques.

[18] The first estimate was made using:

$$\partial H / \partial t_{strain} = b_{40} - F(H(\varepsilon_x + \varepsilon_y) + u(\partial H / \partial x)) \quad (8)$$

[*Paterson*, 1994; p. 257] where b_{40} is the accumulation rate averaged over the 40 year time period (1963–2003) measured using down borehole ^{137}Cs gamma spectrometry and firn core density profiling as described above. The majority of ice core segments extracted from all three sites were intact and ranged from 30 to 50 cm in length, with a diameter assumed to be 2 mm smaller than the inside diameter of the ice core barrel. Density measurements from all sites were estimated to be accurate to $\pm 5\%$ based on measured core lengths and weights. Here ε_x and ε_y are surface strain rates in the directions along flow and transverse to flow, respectively. Strain rates were calculated from repeat differential global positioning system (DGPS) measurements of the magnitude and direction of displacement of four stakes arranged in a 1 km \times 1 km grid determined between spring 2004 and 2005. F was assigned a value of 0.8 (based on *Reeh and Paterson* [1988]) in order

to relate strain rates measured at the ice cap surface to depth-averaged values. Here, u is the downslope velocity derived from repeat DGPS stake measurements and ∂H was calculated over a 1 km distance (∂x) from the ice thickness grid produced by *Dowdeswell et al.* [2004].

[19] The second method used was the “coffee can” technique [*Hamilton and Whillans*, 2000] which derives the long-term rate of thickness change at a single point from the equation:

$$\partial H / \partial t_{cc} = (b_{40} / \rho) + z + u v \quad (9)$$

where b_{40} (positive for accumulation) is the net mass balance averaged over the period from 1963 to 2003, z is the ice submergence velocity derived from precise GPS measurements of a marker anchored 20 m below the ice surface (negative downward), ρ is the firn density at the marker depth, and v is the surface slope measured across one ice thickness in the direction of flow (positive downward). The value of z was calculated as the average of three measurements performed each spring from 2004 to 2007.

[20] The validity of this method relies on the assumption that ρ increases consistently with depth implying that b and z have been relatively constant over the last 40 years or more. To test this, a suite of “coffee cans” were installed at each site in order to determine whether or not a linear relationship between z and $1/\rho$ exists at depths of 20, 16, 12, 8, and 4 m, as would be expected from *Sorge’s Law* [*Hamilton and Whillans*, 2000]. The data from sites 1 and 2 do show such a linear relationship, indicating that compaction rates have not been significantly influenced by recent changes in temperature or precipitation. The “coffee can” method should therefore result in valid calculations of the rate of thickness change at these locations [*Hamilton and Whillans*, 2000]. The upper 20 m of the ice cap at site 3 was composed entirely of ice with a density of 917 kg m^{-3} ; therefore submergence velocity measured at the ice surface was assumed equal to submergence velocity at marker depth. Uncertainties of the “coffee can” measurements are largely a function of the accuracy of the GPS measurements of vertical position, which were $\pm 3, 5, \text{ and } 6 \text{ cm a}^{-1}$ for sites 1, 2, and 3, respectively.

3.3. Rates of Thickness Changes Along Major Outlet Glaciers

[21] Rates of thickness change along five major outlet glaciers (North and South Croker Bay, Southeast 1 and 2, and Fitzroy Glaciers) were computed from the divergence of ice flux between successive gates along the glaciers and the average surface mass balance between these gates:

$$\partial H / \partial t_{Glacier} = [(Q_{InSARg1} - Q_{InSARg2}) / Area_{gLg2}] + SMB_{gLg2} \quad (10)$$

where $g1$ and $g2$ are fluxgates positioned at the up- and down-glacier ends of 5–8 km long glacier segments. Fluxgates were chosen to enclose sections of the glacier that were relatively homogeneous in terms of lateral constraints along the margins. As for (3), Q_{InSAR} ($\text{m}^3 \text{ a}^{-1}$ w.e.) was derived as the product of HV_{InSAR} ($\text{m}^2 \text{ a}^{-1}$) and

Table 2. Volume Change Estimates of All Major Drainage Basins According to Flux Imbalance as Derived in This Study and the Maximum Thickness Area Change Technique as Derived by *Burgess and Sharp* [2004]^a

Basin ID	Volume Change Derived From Flux Imbalance $\times 39$ Years (km^3 w.e.)	Volume Change Derived From Areal Changes 1960–1999 (km^3 w.e.)
9	-1.91 ± 0.19	-1.76 ± 0.21
25	-1.76 ± 0.04	-1.62 ± 0.19
40	-2.46 ± 0.88	-2.56 ± 0.31
37	-2.07 ± 0.05	-1.46 ± 0.18
30	-4.25 ± 0.18	-4.66 ± 0.40
3	-2.07 ± 0.20	-0.66 ± 0.08
15	-11.19 ± 1.44	-8.11 ± 0.62
38	5.62 ± 1.32	2.66 ± 0.33
39	-19.46 ± 1.23	-5.15 ± 0.62
60	-20.75 ± 0.26	-12.19 ± 1.48
Total	-60.33 ± 5.8	-35.47 ± 4.6

^aCells in boldface represent volume changes that agree to within the specified margin of error.

the glacier width ($\text{Width}_{\text{Glacier}}$) (m), where HV_{InSAR} was obtained as an average value across the width of the glacier at each fluxgate. Area_{g1-g2} (m^2) is the area between $g1$ and $g2$ and SMB_{g1-g2} ($\text{m}^3 \text{a}^{-1}$ w.e.) is the average net surface mass balance between fluxgates obtained from *Mair et al.* [2005].

[22] In addition to quantifying the rate of thickness change between fluxgates, equation (10) provides the basis for identifying the main driver behind the measured changes. The relative magnitudes of Term1 and Term2 (as shown in Figures 6b–10b) indicate whether the resultant changes are caused primarily by the prevailing surface mass balance in the region, ice dynamics, or both.

[23] The error associated with equation (10) was estimated as:

$$\sigma(\partial H / \partial t_{\text{Glacier}}) = \sqrt{(\sigma(\text{Term1}))^2 + (\sigma(\text{SMB}))^2} \quad (11)$$

where

$$\sigma \text{Term1} = \left(\sqrt{\sigma Q_{g1}^2 + \sigma Q_{g2}^2} \right) / \text{Area}_{g1-g2} \quad (12)$$

and

$$\sigma(Q) = Q \left(\sqrt{\left(\frac{\sigma(\text{Width})}{\text{Width}} \right)^2 + \left(\frac{\sigma(H)}{H} \right)^2 + \left(\frac{\sigma(V_{\text{InSAR}})}{V_{\text{InSAR}}} \right)^2} \right) \quad (13)$$

Direct measures of surface elevation change along the entire length of the Belcher Glacier, and along a 5 km transect parallel to its terminus (lines NASA_BC and NASA_BF; Figure 2), were computed as the difference between elevations derived from analytical stereo photogrammetry from 1960 aerial photography (ELEV_{1960} ; ± 2 m) and the 2005 ATM data. Individual NASA ATM laser shots (horizontal spacing of ~ 2 m) were interpolated to 20×20 m grid cells (using an inverse distance weighted function) in order to match the resolution of the 1960 DEM. Total error associated with these elevation change

measurements, calculated as the square root of the sum of the squared errors divided by the 45-year time interval between data set acquisitions, was estimated to be $\pm 0.04 \text{ m a}^{-1}$.

4. Results

4.1. Post-1960 Volume Change of the Ice Cap and Its Contribution to Global Sea Level

[24] The average volume loss from the main part of the Devon Island ice cap between 1960 and 1999 derived from the basin-wide calculations was $-60.3 \pm 6 \text{ km}^3$ w.e. ($-5.0 \pm 0.5 \text{ m w.e.}$). This estimate is derived for basins that constitute 78% of the main part of the ice cap. Volume loss from the remaining 22% of the ice cap was estimated as the sum of the volume change attributed to net surface mass balance ($-16.5 \pm 2 \text{ km}^3$ water equivalent) [*Mair et al.*, 2005] and iceberg calving ($-0.014 \pm 0.007 \text{ km}^3$ w.e.) [*Burgess et al.*, 2005]. This equates to a total loss of $-76.8 \pm 7 \text{ km}^3$ w.e. (or $-6.3 \pm 0.6 \text{ m w.e. thinning}$) between 1960 and 1999, or an average annual loss rate of $-1.9 \text{ km}^3 \text{ a}^{-1}$ w.e. (or -0.16 m a^{-1} w.e. thinning) over this period of time. Assuming that the total area of the Earth's oceans is $360 \times 10^6 \text{ km}^2$, this implies that the Devon Island ice cap contributed $+0.21 \pm 0.02 \text{ mm}$ to global sea level between 1960 and 1999. This amounts to approximately 2% of the worldwide input from small ice caps and glaciers based on the current contribution from these sources, estimated to be $+0.59 \text{ mm a}^{-1}$ between 1960 and 2003 [*Dyrgerov and Meier*, 2005].

4.2. Distribution of Volume Change Between Basins

[25] All basins examined in this study lost net volume between 1960 and 1999, except for basin 38 where volume increased by $5.62 \pm 1.32 \text{ km}^3$ w.e. (see Table 2). The greatest losses were from basins 39 and 60 in the southeast region, where volume decreased by $-19.46 \pm 1.23 \text{ km}^3$ and $-20.75 \pm 0.26 \text{ km}^3$ w.e., respectively. Volume also decreased significantly in basin 15 in the northeast region by $-11.19 \pm 1.44 \text{ km}^3$ w.e. Basins 9, 25, 30, 37, 40, and 3 experienced an average net loss of $-2.4 \pm 0.25 \text{ km}^3$ w.e. Among these basins, the greatest ice volume loss occurred from basin 30 ($-4.25 \pm 0.18 \text{ km}^3$ w.e.).

4.3. Distribution of Ice Thickness and Volume Changes Between Accumulation and Ablation Areas and Factors Controlling the Changes Observed

[26] Basin-wide estimates indicate that thickness changes across the accumulation zones of the northern basins (9, 3, and 15) are indistinguishable from zero, while the accumulation zones of basins 30 and 40 along the eastern margin are thinning slightly (Figure 3). Basins 38 and 39 in the southern region are thinning throughout their accumulation zones at rates of $-0.12 \pm 0.12 \text{ m a}^{-1}$ w.e. and $-0.23 \pm 0.11 \text{ m a}^{-1}$ w.e., respectively (Figure 3). In situ measurements indicating near-zero thickness change conditions at site 1 and slight thinning at site 2 in the southwest accumulation zone (Table 3) agree closely with the basin-wide values for this region. The significant thinning estimated for the $1 \times 1 \text{ km}$ grid at site 3 ($-0.23 \pm 0.07 \text{ m a}^{-1}$ w.e.) is likely due to the fact that the easternmost pole in this grid is located in ice that is accelerating eastward toward the

Table 3. Rates of Thickness Change Derived From in Situ Four GPS Measurements Obtained Annually Each Spring Between April 2004 and May 2007 at Three Study Sites in the Southwest Region of the Devon Island Ice Cap

Site	Coffee Can Method (m a^{-1} w.e.)	Thickness Change Across 1 \times 1 km Strain Grid (m a^{-1} w.e.)
1	-0.02 ± 0.03	$+0.03 \pm 0.04$
2	-0.11 ± 0.05	-0.05 ± 0.05
3	$+0.04 \pm 0.06$	-0.23 ± 0.07

South Croker Bay Glacier whereas the remaining poles in the grid are moving southward. Divergent ice motion across the 1×1 km grid thus results in a higher rate of thinning than was estimated from the “coffee can” method at a single point. With the exception of this value, the in situ measurements are likely representative of thickness changes over a broader area because they are located in regions of

low flow rates ($<15 \text{ m a}^{-1}$) where seasonal velocity fluctuations are minimal ($<1 \text{ m a}^{-1}$).

[27] The average rates of thickness change for the ablation zones of basin 39 in the southeast region and basin 3 along the north coast are near zero (Figure 3). In these basins, mass loss due to surface melt is replaced almost entirely by influx across the ELA (see Table 1). In basin 38, flux across the ELA exceeds mass loss due to surface melt resulting in net thickening of the southwest ablation zone by $0.55 \pm 0.22 \text{ m a}^{-1}$ w.e. The ablation zones of the remaining basins in the north and northeast regions (9, 15, and 30) are thinning by -0.14 ± 0.06 , -0.62 ± 0.14 , and $-0.28 \pm 0.07 \text{ m a}^{-1}$ w.e., respectively (Figure 3). Surface lowering by $-0.30 \pm 0.1 \text{ m a}^{-1}$ w.e. as detected along the NASA_EW2 transect (see Figure 2) in basin 40 [Abdalati *et al.*, 2004], agrees with the basin-wide thinning rate of $-0.28 \pm 0.09 \text{ m a}^{-1}$ w.e. in this area. Basins 9, 30, and 40 are losing mass primarily by surface melt (Table 1) whereas more than half of the annual mass loss from basin 15 is by

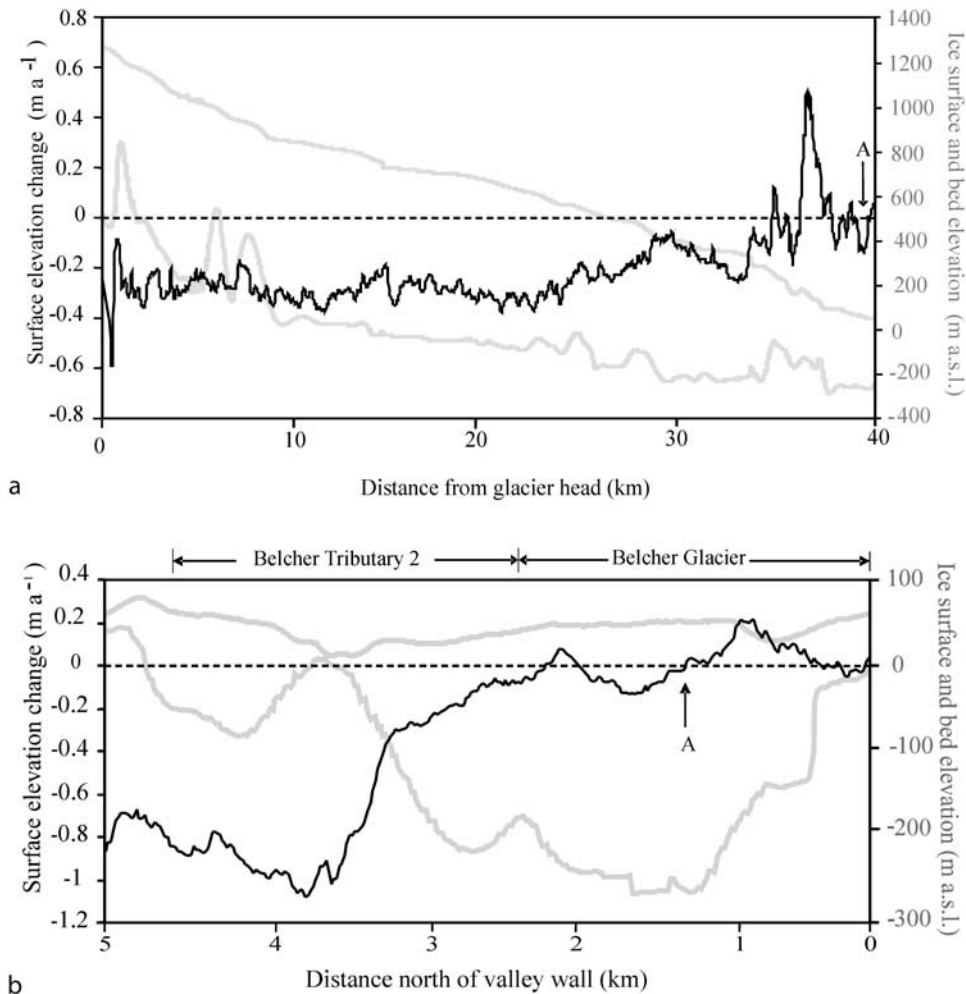


Figure 5. (a) Average annual rate of surface elevation change (black line) along the Belcher Glacier between 1960 and 2005. (b) Average annual rate of surface elevation change (black line) along a 5 km transect running parallel to the terminus of the Belcher Glacier. Ice surface and bed elevations (gray lines) in Figures 5a and 5b were obtained in 2005 from NASA’s Airborne Topographic Mapper and the University of Kansas Coherent Radar Depth Sounder instruments, respectively. “A” indicates the point of intersection between the two transects.

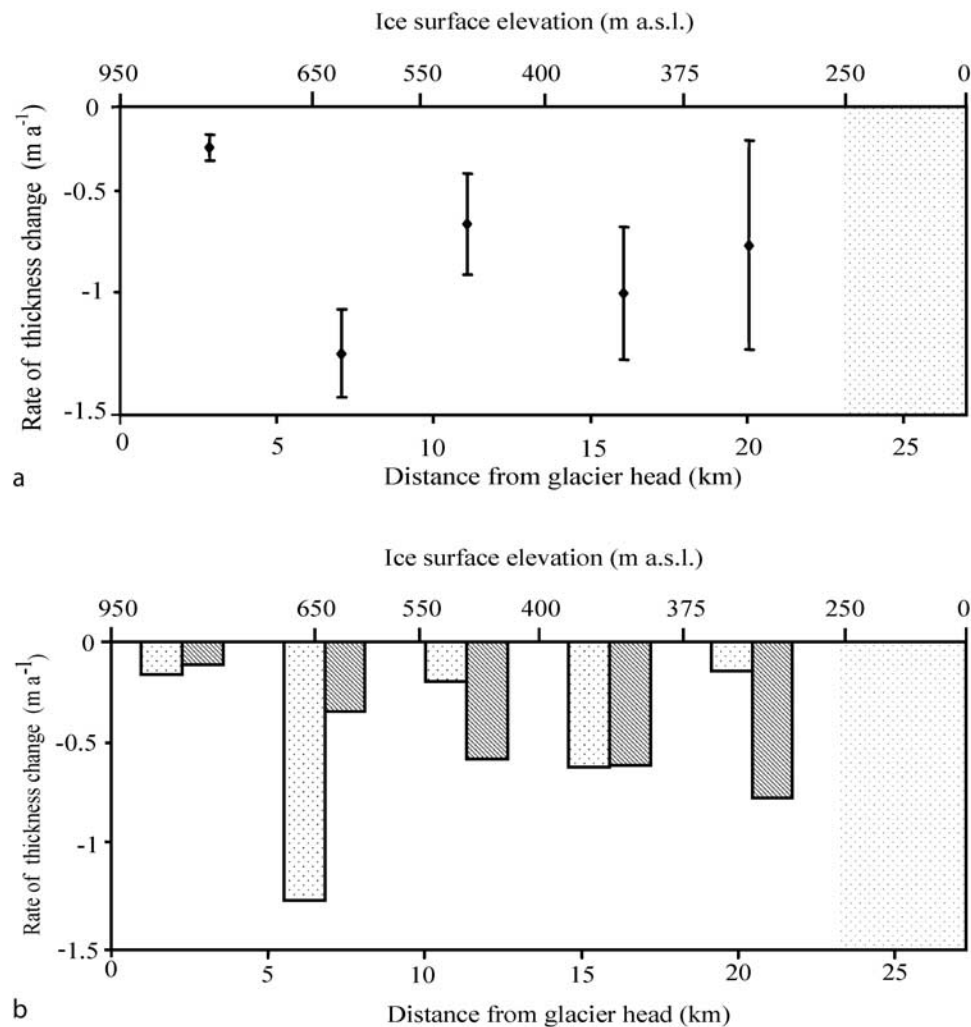


Figure 6. (a) Net thickness change averaged between fluxgates along the Fitzroy Glacier. Values along the top axis indicate the elevation of each fluxgate location. (b) Contributions of surface mass balance (dark shade) and flux divergence (light shade) to net thickness change. The gray stippled area between km 23 and the terminus indicates the region of the glacier where InSar velocity data are not available.

iceberg calving ($-0.21 \text{ km}^3 \text{ a}^{-1}$ w.e.) [Burgess *et al.*, 2005]. Basins 25, 37, and 60 are situated almost entirely below the ELA and experience net losses of -0.045 ± 0.006 , -0.053 ± 0.008 , and $-0.53 \pm 0.042 \text{ km}^3 \text{ a}^{-1}$ w.e., respectively, due primarily to surface melt (see Table 1).

4.4. Relationship Between Basin-Wide Area Changes and Volume Changes Derived From Mass Flux Imbalance

[28] The estimate of volume change for the main portion of the Devon Island ice cap derived from area change measurements [Burgess and Sharp, 2004] is -43 km^3 w.e. compared with $-76.8 \pm 7 \text{ km}^3$ w.e. as derived in this study. There is however a relatively strong relationship ($r^2 = 0.8$) between the two estimates of volume loss for individual basins. Volume changes estimated using the two methods agree to within 1.41, 0.4, and 0.6 km^3 w.e. for basins 3, 30, and 37, and to within measurement uncertainty for basins 9, 25, and 40. The volume-area scaling technique therefore provides a reasonable estimate of volume change for these basins. This is not, however, the case for basins 39, 60, 38,

and 15 where estimates of volume change based on changes in area are lower than the values calculated in this study by 14.31, 8.56, 2.96, and 3.08 km^3 w.e., respectively (see Table 2). Three of these basins are experiencing significant thickness changes due to changes in ice dynamics within either their accumulation (basin 39) or ablation zones (basins 15 and 38) (see below), while basin 60 is thinning throughout due primarily to surface melt. In all of these cases, volume loss is not proportionally reflected in changes at the ice cap margin.

4.5. Longitudinal Patterns of Thickness Change on Outlet Glaciers and Comparison With Thickness Changes at the Basin-Wide Scale

[29] Direct observations of surface elevation change on the Belcher Glacier indicate lowering of the ice surface by $-0.4 \pm 0.04 \text{ m a}^{-1}$ (of ice) along most of its length, with localized thickening near the terminus (Figure 5a). Similarly, elevation change measurements along an across-glacier profile near the glacier terminus indicate slight thickening or near-zero change across the main Belcher

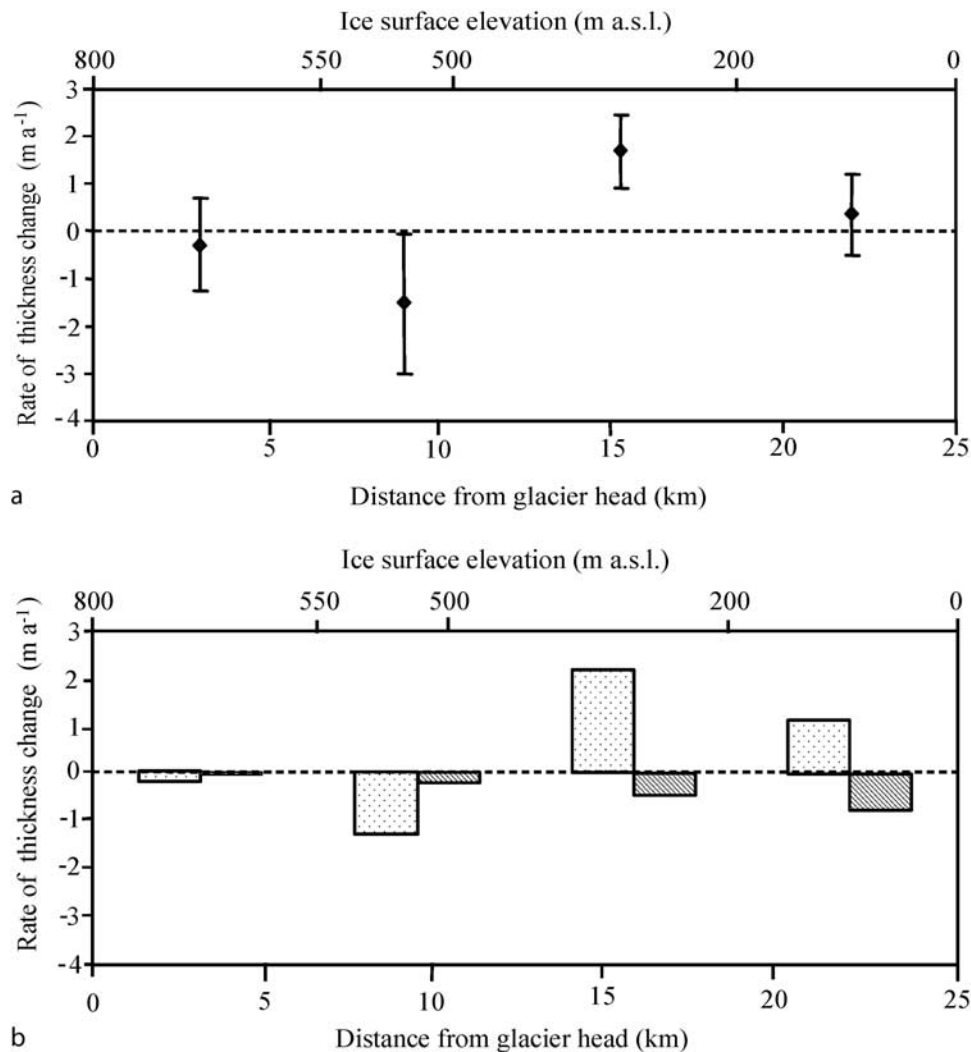


Figure 7. (a) Net thickness change averaged between fluxgates along the North Croker Bay Glacier. Values along the top axis indicate the elevation of each fluxgate location. (b) Contributions of surface mass balance (dark shade) and flux divergence (light shade) to net thickness change.

Glacier channel (Figure 5b). Overall thinning of the ablation zone in basin 15 by $-0.62 \pm 0.14 \text{ m a}^{-1} \text{ w.e.}$ is significantly greater than the average rate of surface lowering along the Belcher Glacier below the ELA ($-0.3 \pm 0.04 \text{ m a}^{-1} \text{ w.e.}$). Since the Belcher Glacier occupies approximately 37% of the ablation zone of basin 15, it is likely that thinning throughout the less dynamic portions of this ablation zone is greater than it is along the main flow unit. This is supported by the higher rate of surface lowering ($-0.8 \pm 0.1 \text{ m a}^{-1}$ of ice) near the terminus in the region of the less active Belcher Tributary 2 Glacier (Figure 5b).

[30] The Fitzroy Glacier is thinning along most of its length, with maximum rates of $-1.2 \text{ m a}^{-1} \text{ w.e.}$ occurring 20 km from the ice front (Figure 6a). The section of this glacier along which thickness changes were computed represents approximately 30% of total area of the ablation zone, which is thinning by $-0.28 \pm 0.07 \text{ m a}^{-1} \text{ w.e.}$ (Figure 3).

[31] In the southwest region, the North and South Croker Bay Glaciers occupy only 18% of the ablation zone of basin 38. Both of these glaciers exhibit near-zero thickness change conditions close to their heads and thinning between 7 and 12 km along these flow units. Thickening by $1.7 \pm 0.7 \text{ m a}^{-1} \text{ w.e.}$ along the lower reaches of the North Croker Bay glacier (Figure 7a) is consistent with, but greater than, the pattern of thickening that prevails throughout the ablation zone of this basin ($0.55 \pm 0.22 \text{ m a}^{-1} \text{ w.e.}$). By contrast, thinning of up to $-2.4 \pm 0.75 \text{ m a}^{-1} \text{ w.e.}$ prevails throughout the lower reaches (<400 m a.s.l.) of the South Croker Bay Glacier (Figure 8a).

[32] In the southeast region (basin 39), thinning by up to $-1 \text{ m a}^{-1} \text{ w.e.}$ along the upper 15 km of the Southeast 1 outlet glacier (Figure 9a) is consistent with, but greater than, basin-wide thinning of this accumulation zone by $-0.23 \pm 0.12 \text{ m a}^{-1} \text{ w.e.}$ (Figure 3). The Southeast 1 and 2 glaciers however are thickening by up to $1 \text{ m a}^{-1} \text{ w.e.}$, approximately 20 km inland from their termini, while their lower-

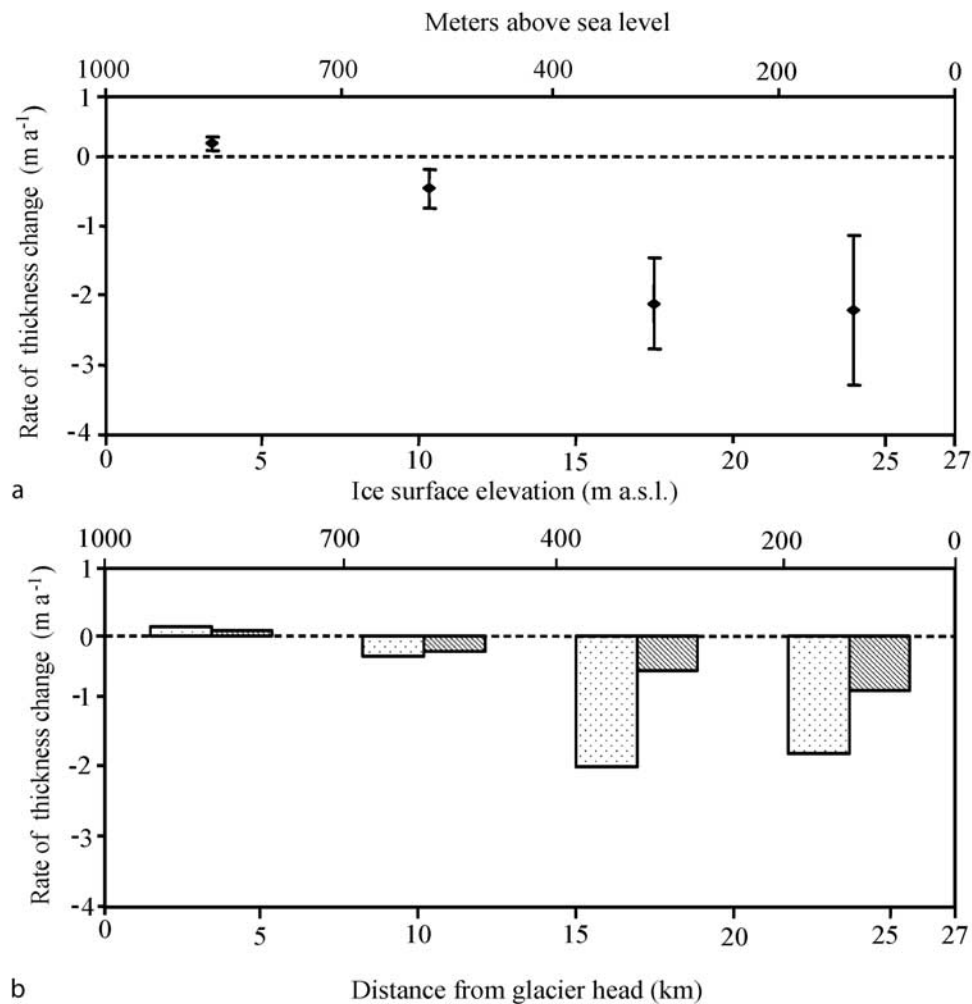


Figure 8. (a) Net thickness change averaged between fluxgates along the South Croker Bay Glacier. Values along the top axis indicate the elevation of each fluxgate location. (b) Contributions of surface mass balance (dark shade) and flux divergence (light shade) to net thickness change.

most reaches are thinning by -1 m a^{-1} w.e. (Figures 9a and 10a). These glaciers occupy approximately 50% of the ablation zone of this basin and draw sufficient mass from higher elevations to offset mass loss due to surface melt below the ELA.

4.6. Evidence for Recent Changes in Flow Dynamics That Have Resulted in Rates of Thinning/Thickening That Are Not Easily Accounted for by Surface Mass Balance

[33] Direct observations of surface elevation change along the Belcher Glacier indicate that the surface of this glacier has been lowering by $-0.35 \pm 0.04 \text{ m a}^{-1}$ of ice, up to and beyond 1400 m a.s.l. (Figure 5a), or approximately 400 m above the long-term ELA. Mass balance data obtained over the past 4 decades from the summit region reveal a near-zero trend in surface mass balance across the Devon Island ice cap above the ELA (1000 m a.s.l.) (R. Koerner, personal communication, 2007). *Colgan and Sharp* [2008], however, do report a negative trend (-0.06 m a^{-1} w.e.) in surface mass balance in this region since the late 1980s. Although this trend may have contributed slightly to

net lowering of the Belcher Glacier, it would not be sufficient to account for the total amount of thinning observed in this study. Most of the surface lowering has therefore likely been dynamically driven and possibly linked to an increased rate of ice flux at lower elevations. In situ measurements of surface mass balance obtained from the northwestern sector of the ice cap (60 km due west of the Belcher Glacier terminus) show a trend toward slightly greater rates of surface ablation below 700 m a.s.l. since 1960. Summer melt below 500 m a.s.l. in this region has increased significantly since the late 1980s (R. Koerner, personal communication, 2007). Thickening of the near-terminus section of the glacier (<300 m a.s.l.) is therefore also likely to be dynamically driven and may be influenced by the recent increase in ice flux from the upper reaches of this glacier.

[34] For the remaining glaciers, dynamically induced thickness changes were identified by comparing the relative contributions of flux divergence and surface mass balance, with the net thickness change between fluxgates. Briefly, a positive (or negative) flux imbalance occurs where flux at the lower gate is greater (or less) than flux at the upper gate

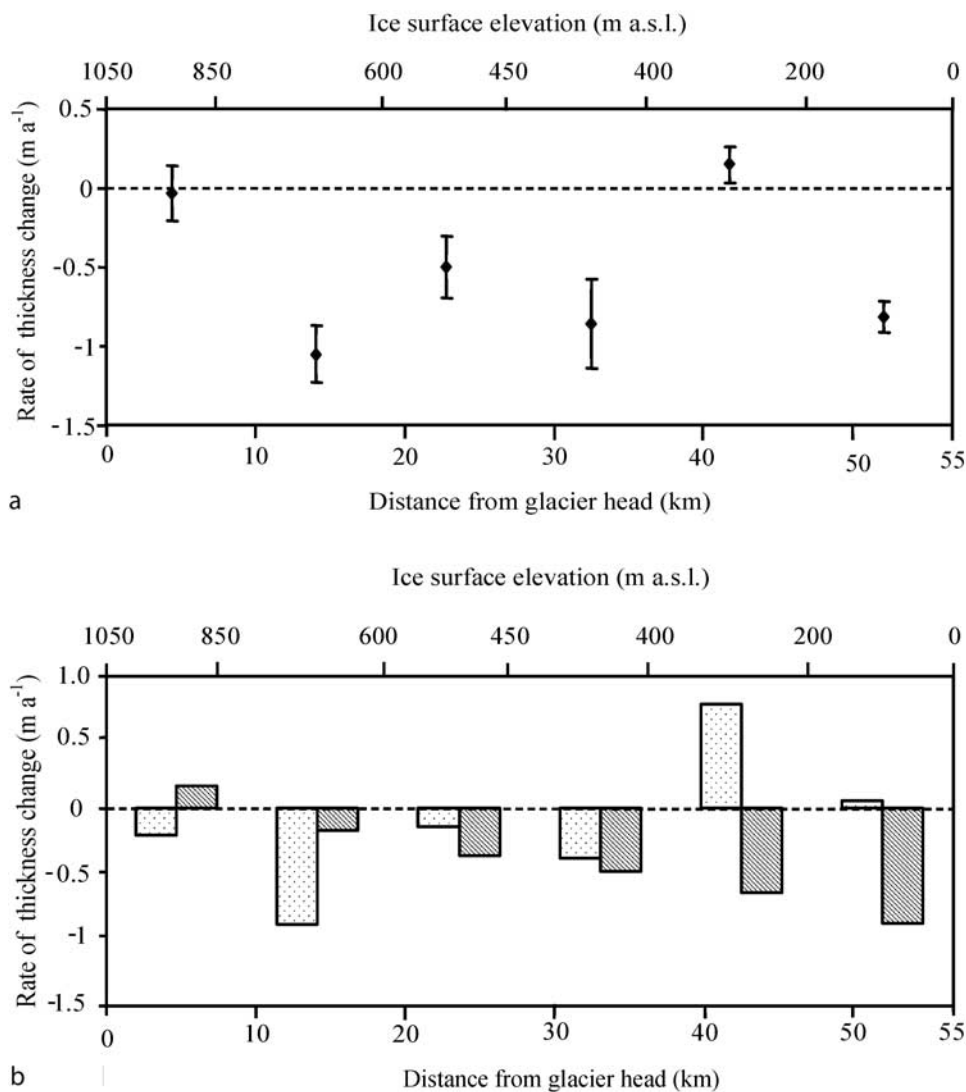


Figure 9. (a) Net thickness change averaged between fluxgates along the Southeast 1 Glacier. Values along the top axis indicate the elevation of each fluxgate location. (b) Contributions of surface mass balance (dark shade) and flux divergence (light shade) to net thickness change.

plus the net surface mass balance between gates. In these situations, flux at the lower gate is enhanced (or inhibited) relative to the net balance integrated over the area between fluxgate locations, leading to dynamically driven thinning (or thickening). Mechanisms influencing variability in the rate of flow along the glaciers examined in this study are discussed in the next section.

[35] Thinning of up to $-1.3 \pm 0.3 \text{ m a}^{-1}$ w.e. within 7 km of the head of the Fitzroy Glacier (Figure 6a) coincides with a positive flux gradient that exceeds local surface ablation rates by a factor of almost three (Figure 6b) suggesting that change within this area is dynamically driven. The limited spatial extent over which the thinning occurs is more suggestive of a local change in ice dynamics than of variability in surface mass balance, which would likely affect a greater spatial region. In the southwest region of the ice cap, thinning near the head of the North Croker Bay Glacier (Figure 7a) appears to be largely attributable to a

positive flux gradient (Figure 7b) that is associated with the acceleration of flow into a bedrock valley. The net surface mass balance at this location is only slightly negative (-0.15 m a^{-1} w.e.) suggesting that thinning is driven primarily by recent increases in the rate of ice flow. Reduced rates of ice flux toward the terminus however are, however, causing dynamic thickening by $1.7 \pm 0.8 \text{ m a}^{-1}$ w.e. and near-zero thickness change where surface mass balance is -0.55 and -0.95 m a^{-1} w.e., respectively (Figure 7b). Along the lower 10 km of the South Croker Bay Glacier (Figure 8a), thinning is probably driven by recent changes in ice dynamics as a positive flux gradient in this segment of the glacier accounts for more than twice the rate of thinning that is attributable to surface mass balance alone (Figure 8b). Increased rates of iceberg calving and terminus advance of this glacier by up to 600 m since 1960 [Burgess and Sharp, 2004] likely represent the main sinks for increased flux from this glacier.

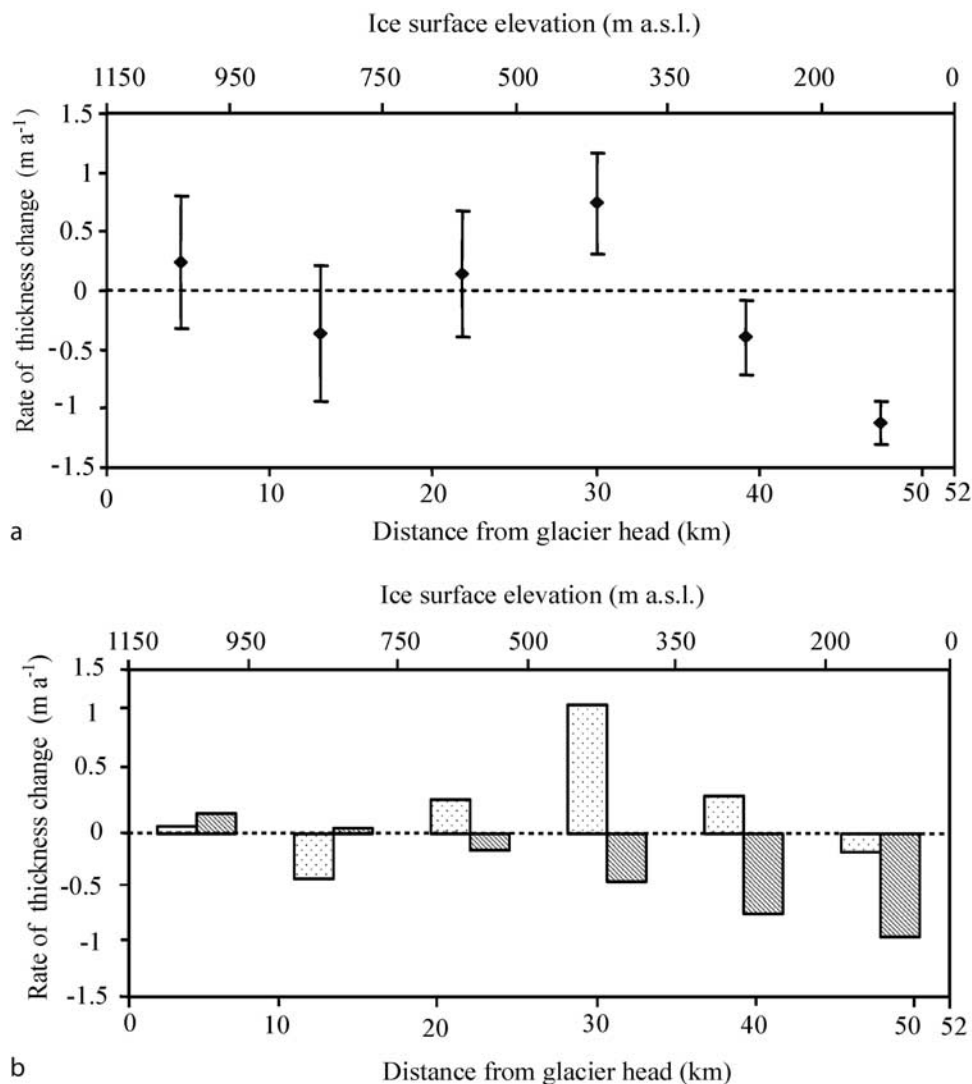


Figure 10. (a) Net thickness change averaged between fluxgates along the Southeast 2 Glacier. Values along the top axis indicate the elevation of each fluxgate location. (b) Contributions of surface mass balance (dark shade) and flux divergence (light shade) to net thickness change.

[36] The general patterns of thickness change along those sections of the Southeast 1 and 2 Glaciers above 350 m a.s.l. are indicative of dynamically induced changes in ice thickness, whereas thinning near the glacier termini is due almost entirely to surface melt. Net thinning by $-1.1 \pm 0.2 \text{ m a}^{-1}$ w.e. between 10 and 20 km down-glacier from the head of the Southeast 1 Glacier is associated with a positive flux gradient (Figure 9a) that causes thinning at a rate that is roughly 5 times greater than that due to the local surface mass balance (Figure 9b). A positive flux gradient also occurs near the head of the Southeast 2 Glacier (Figure 10b), but uncertainties in this estimate, combined with slightly positive surface mass balance make net thickness change in this area indistinguishable from zero (Figure 10a). The lower reaches of the Southeast 1 and 2 Glaciers both experience net thickening in the region 20 km up-glacier of their termini (Figures 9a and 10a) where faster flowing ice from higher elevations runs into slower flowing ice at lower elevations (Figure 11). Decelerating ice flow along

these glaciers results in dynamic thickening that more than compensates for mass loss due to local net surface ablation.

5. Discussion

[37] The patterns of dynamic thickness change identified in this study provide some important clues concerning the mechanisms responsible for nonsteady flow along many of the outlet glaciers that drain the Devon Island ice cap. As mentioned above, net surface lowering along the Belcher Glacier between 300 and 1400 m a.s.l. most likely reflects an excess of outflow over net accumulation from this glacier system due to recent increases in the rate of ice flow. Analysis of aerial photographs and field observations reveal a system of meltwater channels that begin at 1500 m a.s.l. and terminate in crevasse fields or moulins at lower elevations. These features may provide surface water with access to the glacier bed, thus enhancing flow through basal lubrication or by reducing the effective ice overburden

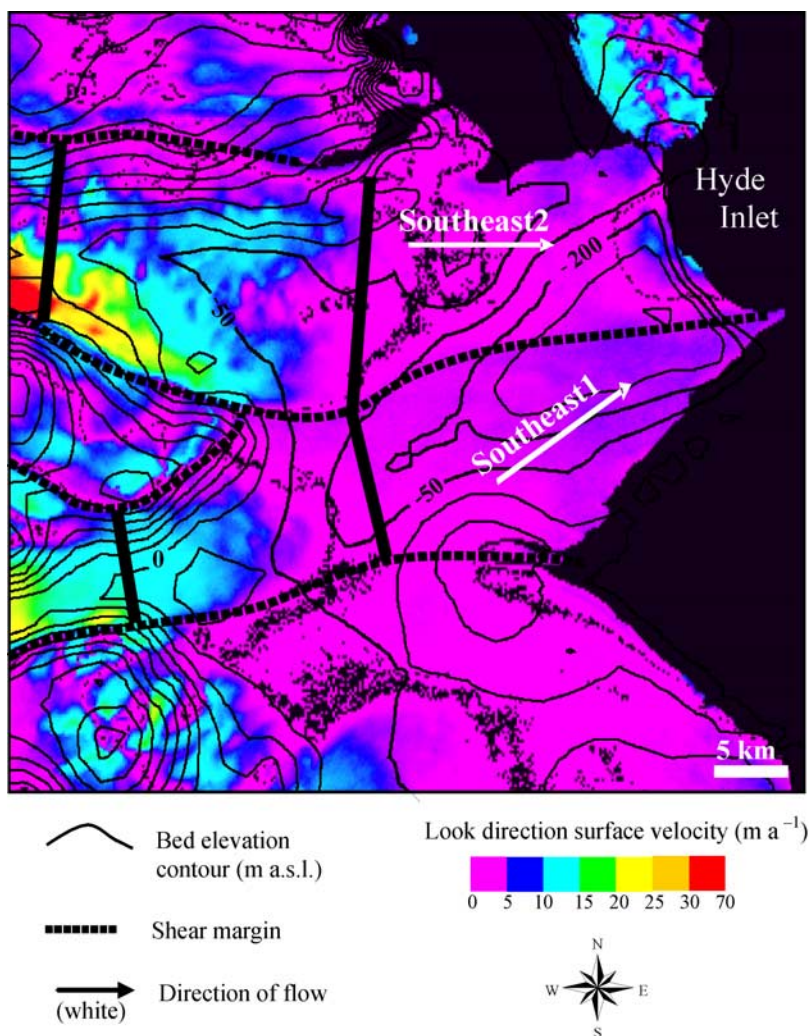


Figure 11. Bedrock topography and InSAR derived surface velocities in the look direction of the satellite across the terminus region of the Southeast 1 and 2 outlet glaciers. The heavy lines perpendicular to flow demarcate the zones of dynamic thickening along the Southeast 1 and 2 Glaciers, respectively. The transition from warm- to cold-based ice as inferred by *Burgess et al.* [2005] corresponds roughly to the color transition from dark blue to purple in the direction of glacier flow.

pressure. Predominant thickening near the terminus of the Belcher Glacier is likely driven by compressive forces as it experiences a sharp reorientation of flow and converges with the slower moving Belcher Tributary 2 glacier flowing in from the west (Figure 12). Lateral compression is inferred from a reduction in the width of the channel along the eastward flowing segment by ~ 500 m relative to the channel up-glacier from the curve. Narrowing of the glacier channel may induce higher ice velocities, which reach ~ 300 m a^{-1} along this eastward flowing segment of the glacier [*Burgess et al.*, 2005]. Enhanced flow within this segment occurs over topographic ridges at the glacier bed (Figure 5a) which would result in longitudinal compression and likely contribute to the thickening that is observed at these locations. Predominant thickening of the near-terminus region of the Belcher Glacier, combined with the fact that there has been minimal net change in position of this margin since 1960 (Figure 12), suggests that the stability of this ice front has not been significantly affected by recent

climate warming. By contrast, significant thinning across the less dynamic (and thinner; see Figure 5b) portions of the Belcher Tributary 2 glacier reflects the vulnerability of this margin to the effects of floatation and retreat due to calving. Thinning across this northern segment of the cross-flow profile is likely due to the fact that ice flux to this part of the terminus is insufficient to replace mass loss due to surface melt. Factors similar to these may be responsible for the ~ 3 km^2 portion of ice lost sometime between 1984 and 1999 from the northern part of this margin (Figure 12). The timing of this event was determined from analysis of video from an aerial survey conducted in 1983 [*Taylor and Frobel*, 1984] and the 1999 Landsat ETM+ image used in this study.

[38] The patterns of ice dynamics and thickness change along the Southeast 1 and 2 Glaciers suggest that nonsteady flow in this region may be controlled by a surge-type mechanism. Thinning along the upper reaches of the Southeast 1 (and possibly Southeast 2) Glacier(s) coincides with

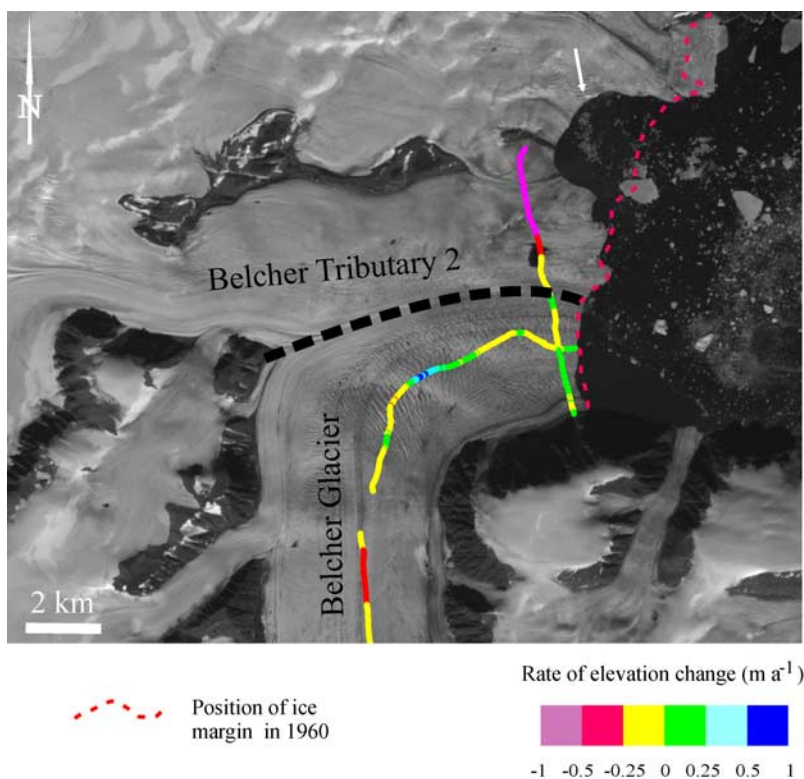


Figure 12. Rates of surface elevation change (m a^{-1}) in the Belcher Glacier terminus region (1960–2005) overlaid on a July 1999 Landsat ETM+ panchromatic orthoimage. Arrow points to a $\sim 3 \text{ km}^2$ portion of ice that calved sometime between 1983 and 1999.

maximum flow rates along these glaciers. These sectors may represent the actively surging portions of the glaciers where dynamic lowering of the ice surface is occurring. Maximum thickening on the other hand occurs where “fast” flowing ice from the upper reaches of these glaciers runs into near-stagnant ice at lower elevations (Figure 11). These zones of thickening coincide with strong longitudinal velocity gradients that likely represent surge fronts propagating into the slower moving ice at lower elevations [Sharp *et al.*, 1988; Murray *et al.*, 1998]. The presence of looped moraines and degraded flow stripes near the stagnant margin of these glaciers provides evidence that fast flow did extend into this region in the past. This near-stagnant terminus region, which is currently thinning, presumably has yet to be reactivated by the surge.

[39] The estimate of total volume change of the main part of the Devon Island ice cap of -32 km^3 water equivalent over the past 40 years derived from extrapolation of airborne laser altimetry measurements [Abdalati *et al.*, 2004], is significantly lower than our estimate of $-76 \pm 7 \text{ km}^3$ water equivalent. This may reflect a difference in thinning rates between the period covered by our assessment and that covered by the NASA measurements, but it may also derive from the fact that the NASA transects did not sample the regions where the most significant changes are occurring. The NASA transects from which these changes were derived (NASA_EW1, NASA_EW2, and NASA_NS1; Figure 2) are confined primarily to the main east-west divide and the western lobe, which are relatively inactive regions. The most significant changes however are occurring within the accumulation zone of the southeast region, the lower reaches of the

South Croker Bay Glacier, the ablation zone of basin 15 and in the low-lying basins that are almost entirely below the current ELA such as basin 60 (see Table 2). Since these areas are not sampled by the airborne laser altimetry surveys, estimates of volume change based on the results of those surveys may be too low.

[40] In many ways, the pattern of thickness changes observed over the Devon Island ice cap is similar to that measured over the Greenland ice sheet [Thomas *et al.*, 2001; Thomas *et al.*, 2005; Luthcke *et al.*, 2006; Stearns and Hamilton, 2007; Joughin *et al.*, 2008]. The broad scale pattern of thickness change over both Greenland and the Devon Island ice cap is one of near balance at high elevations and thinning near the ice cap margins [Krabill *et al.*, 2000]. Accumulation zone thinning rates of -29 cm a^{-1} and -23 cm a^{-1} do, however, occur in the southeast regions of Greenland [Thomas *et al.*, 2000] and Devon respectively. In both cases, these basins are likely influenced significantly by the behavior of the major outlet glaciers that drain them (King Christian IV, Pikiutdleg, and Helheim for Greenland [Abdalati *et al.*, 2001] and Southeast 1 and 2 for Devon). Dynamic thinning occurs well into the accumulation zones along these glaciers. Finally, several major tidewater glaciers that drain the Greenland Ice Sheet (Rink Isbrae, Kangerdlugsuup, Kjer, King Oscar, Humboldt North, Eqalorutsit East, Eqalorutsit West, Storsstrommen North) have zones of dynamic thinning similar to those along sections of the Belcher and South Croker Bay Glaciers on Devon. As on Greenland, some regions of surface lowering within the Devon Island ice cap appear to be attributable to recent changes in ice dynamics. Mass

loss due to these changes must therefore be accounted for to provide a reliable basis for assessing volume change of the ice mass as a whole [Abdalati *et al.*, 2001].

6. Conclusions

[41] Indirect measurements of rates of thickness change performed across the Devon Island ice cap, Nunavut, Canada reveal significant variability in the sign and magnitude of thickness changes between basins over the period from 1960 to 2003. The accumulation zones of the south and east regions of the ice cap are thinning slightly while rates of thickness change across the accumulation zones of the northern basins are indistinguishable from zero. Maximum thinning by $-0.23 \pm 0.11 \text{ m a}^{-1}$ w.e. occurs in the accumulation zone of the southeast basin. Thickness changes indistinguishable from zero prevail in the ablation zone of the southeast region while the southwest ablation zone is thickening by $0.55 \pm 0.22 \text{ m a}^{-1}$ w.e. The ablation zones of most basins in the northern region are thinning slightly with maximum rates of -0.62 m a^{-1} w.e. in the northeast sector. Overall, the main part of the Devon Island ice cap has decreased in volume by $-76.8 \pm 7 \text{ km}^3$ w.e. between 1963 and 2000, resulting in a net contribution of $+0.21 \pm 0.02 \text{ mm}$ to global sea level rise over this period of time. This estimate is up to $\sim 44\%$ greater than independent estimates based on volume-area scaling methods and surface mass balance alone, suggesting that ice dynamics must be included in models aimed at assessing the net mass balance of a large ice cap as a whole.

[42] Along glacier thickness change measurements suggest that all of the outlet glaciers examined in this study exhibit nonsteady, transient flow controlled by mechanisms operating either internally or externally to these systems. Thinning by $-0.35 \pm 0.04 \text{ m a}^{-1}$ of ice along almost the entire length of the Belcher Glacier may be an indirect result of recent warming trends that have occurred over the past 25 years. Dynamic thickening of the Belcher Glacier terminus has probably stabilized this tidewater margin, making it relatively insensitive to recent climate warming. The pattern of thickness change along the Southeast 1 and 2 outlet glaciers, combined with the presence of looped moraines and flow stripes on the surfaces of their near-stagnant termini suggest that these glaciers are characterized by surge-type flow, thus they are likely controlled by mechanisms internal to these systems. The diversity of patterns and rates of thickness change across the Devon Island ice cap suggests a complex interplay exists between changes in ice flow behavior and mass balance.

[43] This study provides insight into the impact of ice dynamics on changes in geometry and net mass balance of a high Arctic ice cap. A major drawback of recent efforts to predict the response of ice caps and glaciers to climate warming is that only changes in volume due to changes in surface mass balance are taken into account [e.g., IPCC, 2007]. Although the rates of volume change associated with changes in the flow of these glaciers are much less than those observed recently over Greenland, they are nonetheless significant for the overall balance of these ice masses.

[44] **Acknowledgments.** This work was supported by grants from NSERC (Canada) and the Meteorological Service of Canada (CRYSYS

program) to M. Sharp. D. Burgess received an IPS-2 scholarship from NSERC and Land Data Technologies Inc. and grants from the Canadian Circumpolar Institute and Northern Scientific Training Program (Department of Indian and Northern Affairs Canada). Gridded ice thickness data set provided by J. Dowdeswell were collected under NERC grant GR3/12469 and the EU SPICE project. Ice thickness profile data were obtained from S.P. Gogenini at the Center for Remote Sensing of Ice Sheets (CRISIS), University of Kansas. Airborne Laser Altimetry data were obtained from Bill Krabill of NASA Wallops Flight Facility, Virginia, U.S.A. Logistical support in the field was provided by the Polar Continental Shelf Project, Natural Resources Canada. We thank the Nunavut Research Institute and the hamlets of Grise Fiord and Resolute Bay for their permission to conduct this research on the Devon Island ice cap. Finally, we thank A. Arendt for many insightful comments on this paper.

References

- Abdalati, W., W. Krabill, E. Frederick, S. Manizade, C. Martin, J. Sonntag, R. Swift, R. Thomas, W. Wright, and J. Yungel (2001), Outlet glacier and margin elevation changes: Near-coastal thinning of the Greenland Ice Sheet, *J. Geophys. Res.*, *106*(D24), 33,729–33,741, doi:10.1029/2001JD900192.
- Abdalati, W., W. Krabill, E. Frederick, S. Manizade, C. Martin, J. Sonntag, R. Swift, R. Thomas, J. Yungel, and R. Koerner (2004), Elevation changes of ice caps in the Canadian Arctic Archipelago, *J. Geophys. Res.*, *109*, F04007, doi:10.1029/2003JF000045.
- Budd, W. F., and R. C. Warner (1996), A computer scheme for rapid calculations of balance-flux distributions, *Ann. Glaciol.*, *23*, 21–27.
- Burgess, D. O., and M. J. Sharp (2004), Recent changes in areal extent of the Devon Island ice cap, Nunavut, Canada, *Arct. Antarct. Alp. Res.*, *36*(2), 261–271, doi:10.1657/1523-0430(2004)036[0261:RCIAEO]2.0.CO;2.
- Burgess, D. O., M. J. Sharp, D. W. F. Mair, J. A. Dowdeswell, and T. J. Benham (2005), Flow dynamics and iceberg calving rates of the Devon Island ice cap, Nunavut, Canada, *J. Glaciol.*, *51*(173), 219–238, doi:10.3189/172756505781829430.
- Colgan, L., and M. Sharp (2008), Combined oceanic and atmospheric influences on net accumulation on Devon Ice Cap, Nunavut, Canada, *J. Glaciol.*, *54*(184), 28–40, doi:10.3189/002214308784409044.
- Dowdeswell, J. A., T. J. Benham, M. R. Gorman, D. Burgess, and M. Sharp (2004), Form and flow of the Devon Island ice cap, Canadian Arctic, *J. Geophys. Res.*, *109*, F02002, doi:10.1029/2003JF000095.
- Dyrugerov, M. B., and M. F. Meier (2005), *Glaciers and the Changing Earth System: A 2004 Snapshot*, 117 pp., Univ. of Colo. Inst. of Arctic and Alpine Res., Boulder, Colo.
- Hamilton, G. S., and I. M. Whillans (2000), Point measurements of mass balance of the Greenland Ice Sheet using precision vertical Global Positioning System (GPS) surveys, *J. Geophys. Res.*, *105*(B7), 16,295–16,301, doi:10.1029/2000JB900102.
- Intergovernmental Panel on Climate Change (2007), *Climate Change 2007: The Physical Science Basis: Contribution of Working Group I to the Fourth Assessment Report of the Intergovernmental Panel on Climate Change*, edited by S. Solomon *et al.*, Cambridge Univ. Press, New York.
- Joughin, I. J., I. Howat, R. B. Alley, G. Ekstrom, M. Fahnestock, T. Moon, M. Nettles, M. Truffer, and V. C. Tsai (2008), Ice-front variation and tide-water behaviour on Helheim and Kangerdlugssuaq Glaciers, Greenland, *J. Geophys. Res.*, *113*, F01004, doi:10.1029/2007JF000837.
- Koerner, R. (1970), Mass balance of the Devon Island ice cap, Northwest Territories, Canada, 1961–66, *J. Glaciol.*, *6*(45), 383–392.
- Koerner, R. (1977), Ice thickness measurements and their implications with respect to past and present ice volumes in the Canadian High Arctic ice caps, *Can. J. Earth Sci.*, *14*, 2697–2705.
- Koerner, R. (2002), Glaciers of the High Arctic Islands, in *Satellite Image Atlas of Glaciers of the World. Glaciers of North America—Glaciers of Canada*, edited by R. S. Williams Jr. and J. G. Ferrigno, *U.S. Geol. Surv. Prof. Pap.*, *1386-J-1*, 111–146.
- Krabill, W., W. Abdalati, E. Frederick, S. Manizade, C. Martin, J. Sonntag, R. Swift, R. Thomas, W. Wright, and J. Yungel (2000), Greenland Ice Sheet: High-elevation balance and peripheral thinning, *Science*, *289*, 428–429, doi:10.1126/science.289.5478.428.
- Krabill, W., P. Gogenini, and M. N. Demuth (2006), Glacier elevation and ice thickness data derived from Airborne LiDAR and Ice Penetrating RaDAR surveys over the reference monitoring glaciers and ice caps of the Canadian Arctic Islands, 2005, 2006, Geol. Surv. of Canada, Ottawa, Ontario, Canada.
- Luthcke, S. B., H. J. Zwally, W. Abdalati, D. D. Rowlands, R. D. Ray, R. S. Nerem, F. G. Lemoine, J. J. McCarthy, and D. S. Chinn (2006), Recent Greenland ice mass loss by drainage system from satellite gravity observations, *Science*, *314*, 1286–1289, doi:10.1126/science.1130776.

- Mair, D. W. F., D. O. Burgess, and M. J. Sharp (2005), Thirty-seven year mass balance of the Devon Island ice cap, Nunavut, Canada determined by shallow ice coring and melt modeling, *J. Geophys. Res.*, *110*, F01011, doi:10.1029/2003JF000099.
- Murray, T., J. A. Dowdeswell, D. J. Drewry, and I. Frearson (1998), Geometric evolution and ice dynamics during a surge of Bakaninbreen, Svalbard, *J. Glaciol.*, *44*(147), 263–272.
- Paterson, W. S. B. (1994), *The Physics of Glaciers*, 3rd ed., Elsevier, Oxford, U. K.
- Reeh, N., and W. S. B. Paterson (1988), Application of a flow model to the ice-divide region of Devon Island Ice Cap, Canada, *J. Glaciol.*, *34*(116), 55–63.
- Rignot, E., and X. Kanagaratnam (2006), Changes in the velocity structure of the Greenland Ice Sheet, *Science*, *311*, 986–987, doi:10.1126/science.1121381.
- Sharp, M., W. Lawson, and R. S. Anderson (1988), Tectonic processes in a surge-type glacier, *J. Struct. Geol.*, *10*, 499–515, doi:10.1016/0191-8141(88)90037-5.
- Stearns, L. A., and G. S. Hamilton (2007), Rapid volume loss from two East Greenland outlet glaciers quantified using repeat stereo satellite imagery, *Geophys. Res. Lett.*, *34*, L05503, doi:10.1029/2006GL028982.
- Taylor, R. B., and D. Frobé (1984), Coastal surveys, Jones Sound, District of Franklin, in *Current Research, Part B, Geol. Surv. Can. Pap.*, *84-1B*, 25–32.
- Thomas, R. H., T. Akins, B. Csatho, M. Fahnestock, P. Gogineni, C. Kim, and J. Sonntag (2000), Mass balance of the Greenland Ice Sheet at high elevations, *Science*, *289*, 426–429, doi:10.1126/science.289.5478.426.
- Thomas, R. H., et al. (2001), Program for Arctic regional climate assessment (PARCA): Goals, key findings, and future directions, *J. Geophys. Res.*, *106*(D24), 33,691–33,705, doi:10.1029/2001JD900042.
- Thomas, R., E. Frederick, W. Krabill, S. Manizade, C. Martin, and A. Mason (2005), Elevation changes on the Greenland ice sheet from comparison of aircraft and ICESat laser-altimeter data, *Ann. Glaciol.*, *42*, 77–82, doi:10.3189/172756405781813050.

D. Burgess, Canada Centre for Remote Sensing, 588 Booth Street, Ottawa, ON K1A 0Y7, Canada. (david.burgess@nrcan.gc.ca)

M. J. Sharp, Department of Earth and Atmospheric Sciences, University of Alberta, Edmonton, AB T6G 2E3, Canada.